

Orbital period changes in RW CrA, DX Vel and V0646 Cen

I.M. Volkov^{1,2}, D. Chochol¹, J. Grygar³, M. Mašek³ and J. Juryšek³

¹ *Astronomical Institute of the Slovak Academy of Sciences
059 60 Tatranská Lomnica, The Slovak Republic, (E-mail: volkov@ta3.sk,
chochol@ta3.sk)*

² *Sternberg Astronomical Institute, Moscow University, Universitetskij Ave.
13, 119992 Moscow, Russia, (E-mail: hwp@yandex.ru)*

³ *Institute of Physics, The Czech Academy of Sciences, 182 21 Praha,
The Czech Republic, (E-mail: grygar@fzu.cz)*

Received: May 5, 2017; Accepted: June 1, 2017

Abstract. We aim to determine the absolute parameters of the components of southern Algol-type binaries with deep eclipses RW CrA, DX Vel, V0646 Cen and interpret their orbital period changes. The data analysis is based on a high quality Walraven photoelectric photometry, obtained in the 1960-70s, our recent CCD photometry, ASAS (Pojmanski, 2002), and Hipparcos (Perryman et al., 1997) photometry of the objects. Their light curves were analyzed using the PHOEBE program with fixed effective temperatures of the primary components, found from disentangling the Walraven ($B - U$) and ($V - B$) colour indices. We found the absolute parameters of the components of all three objects. All reliable observed times of minimum light were used to construct and analyze the Eclipse Time Variation (ETV) diagrams. We interpreted the ETV diagrams of the detached binary RW CrA and the semi-detached binary DX Vel by a Light-Time Effect (LITE), estimated parameters of their orbits and masses of their third bodies. We suggest a long term variation of the inclination angle of both eclipsing binaries, caused by a non-coplanar orientation of their third body orbits. We interpreted the detected orbital period increase in the semi-detached binary V0646 Cen by a mass transfer from the less to more massive component with the rate $\dot{M} = 6.08 \times 10^{-9} M_{\odot}/\text{yr}$.

Key words: stars: binaries: eclipsing – stars: binaries (including multiple): close – stars: mass-loss – stars: fundamental parameters

1. Introduction

Algol-type stars are eclipsing binaries with spherical or ellipsoidal components, characterized by light curves (LCs) in which it is possible to specify the beginning and end of the eclipses. If the light between eclipses changes due to the gravitational deformations we can estimate the mass ratio of the components. The analysis of multicolour LCs of Algols provides the absolute parameters of their components. The parameters of the components, derived from their LCs, allow

to specify the evolutionary status of the eclipsing binaries. Algols are detached, if both components are inside corresponding Roche-lobes and semi-detached if one of the components fills its corresponding Roche-lobe and transfers the matter to the companion. The orbital period can change either due to the mass transfer between the components, mass loss from the system, quadrupole moment variations or multiplicity of the systems (Budding & Demircan, 2007). One of the aims of our paper is to interpret pronounced long-term orbital period changes in the studied binaries, firstly found in our investigation, by the mechanism, which is determining for every system.

We would like to note that the unusual colour changes in minima resulted in discovery of the third body in V0577 Oph system (Volkov, 1990; Volkov & Volkova, 2010) and EQ Boo (Volkov et al., 2011, 2012). In V0974 Cyg we first found the LITE and then discovered the presence of the third body in colour indices (Volkova & Volkov, 2011).

Due to the lack of spectroscopic orbits of our objects, we applied in Section 4 the method described by Khaliullin (1985) for investigation of the eclipsing binary V0541 Cyg. This approach is supported by the agreement of the mass ratio of the components of V0541 Cyg $q = 0.97$ with the value of $q = 0.9681(40)$ recently found from radial velocity curves of the components by Torres et al. (2017). The absolute parameters, estimated by the method described in Khaliullin (1985) such as semi-major axes, radii and masses can only be considered as preliminary. Nevertheless, the positions of components of the studied binaries satisfy the diagrams given at the end of this article.

2. Available observational material and previous studies

The Algol-type binaries RW CrA, DX Vel and V0646 Cen were observed in 1965, 1978 and 1968, respectively by C.J. van Houten using the 90-cm Dutch telescope equipped with the simultaneous *VBLUW* photometer of Walraven, at the Leiden Southern Station, Broederstroom, South Africa. Multicolour Walraven photometry of all 3 objects was published by van Houten et al. (2009).

We compiled all available photometry of these objects including the data from the Hipparcos and ASAS all-sky surveys and added our own CCD photometry of the objects, obtained in 2012-16 by FRAM (Photometric Robotic Atmospheric Monitor): a 0.3m Schmidt-Cassegrain telescope, installed at the Pierre Auger Observatory (Collaboration, 2015) located in Argentina near the town of Malargüe and operated by the Institute of Physics, Czech Academy of Sciences. For more details, see Prouza et al. (2010) and Ebr et al. (2014). The telescope FRAM works in a fully automatic mode using the RTS2 software system (Kubánek et al., 2004) as part of the atmospheric monitoring program of the Pierre Auger Observatory. The telescope is equipped with the CCD camera G2-1600 of Moravian Instruments and Bessel set of filters. The observations

were acquired in the standard BVR_CI_C system. We also used old photographic data to extend the timescale of observations to nearly 80 years.

The eclipsing binary RW CrA (HD 163726, $P = 1.68$ days, $V = 9.56$, B8/A0 III) was discovered by Gaposchkin (1932) and observed episodically since that time. The only solution of the RW CrA LCs was published by Grygar & Horak (1980), based on unpublished van Houten's observations in the Walraven system obtained in 1965. Photometric elements $i, r_1, r_2, u, L_1, L_2, L_3$ were found by the limb-darkening scan technique method developed by Horak (1975). The main feature of the solution was a large amount of the third light L_3 that reached maximum 24% in a B_W passband. The authors did not find any plausible explanation of its existence.

The eclipsing binary DX Vel (HD 297655, $P = 1.12$ days, $V = 10.2$, A5) was discovered photographically by Hoffmeister (1949). The first photographic LC was published by van Houten (1950). Budding et al. (2004) listed the object as a detached or semidetached binary. Due to the fact that the primary component is located in the δ Scuti region of the Cepheid instability strip, it was included by Soydugan et al. (2006) to the list of semidetached candidates for pulsations. However, all available photometry of the object did not confirm the appearance of the δ Scuti pulsations. Our previous investigation of the positions of all available primary minima times in the ETV diagram revealed their changes that can be approximated either by a parabola, or by the LITE orbit (Volkov et al., 2013). Our new investigation presented here confirms the LITE orbit.

The eclipsing binary V0646 Cen (HD 100987, $P = 2.25$ days, $V = 9.12$, B8 IV) was discovered by O'Connell (1951). O'Connell (1956) published the parameters of the system based on his own photographic LC.

All 3 systems are listed in the catalogues of Brancewicz & Dworak (1980) and Budding et al. (2004). In the catalogue of Malkov et al. (2006) RW CrA and V0646 Cen are indicated as semidetached systems.

3. Disentangling of colour indices, two-colours diagrams and determination of temperatures of the components

The most important parameter for analysis of the LCs of the binaries are temperatures of the components, that can be found in the following way. The colour indices of the light loss in primary and secondary minima were calculated directly from the LCs in the Walraven system in different passbands without any additional assumptions. Observed colour indices of the primary and secondary components, presented in Table 1, were dereddened using a two-colour $(B - U)_W, (V - B)_W$ diagram. Calculated "pure" colour indices were used for determination of the temperatures of the components using the well-known calibrations.

The observed and dereddened position of the components of RW CrA in the two colour diagram is shown in Fig. 1. The interstellar reddening in the

Walraven system is $E(V - B)_W = 0.0261$. We converted the Walraven index $(V - B)_W$ into the Johnson $(B - V)_J$ one using the expression given in Pel (1980):

$$\begin{aligned} V_J &= 6.879 - 2.5(V_W + 0.068(V - B)_W), \\ (B - V)_J &= 2.626(V - B)_W - 0.5(V - B)_W^2 - 0.008, \end{aligned} \quad (1)$$

and obtained $E(B - V)_J = 0.07 \pm 0.01$. We derived dereddened indices $(B - V)_{0J} = -0.080$ corresponding to $T_1 = 11100$ K, Sp = B8.5 using the Flower (1996) and Popper (1980) calibrations and $(V - B)_{0W} = 0.1802$, corresponding to $T_2 = 6500$ K, Sp = F5 using the Lub & Pel (1977) calibration.

The other possibility to find the temperatures of the components is to use Strömgren $uvby, \beta$ photometry in minima and on the plateau by Wolf & Kern (1983):

$$\begin{aligned} \text{Primary: } b - y &= 0.031 \pm 0.01, m1 = 0.088 \pm 0.01, c1 = 0.837 \pm 0.01. \\ \text{Secondary: } b - y &= 0.342 \pm 0.01, m1 = 0.136 \pm 0.01, c1 = 0.270 \pm 0.01. \end{aligned}$$

We obtained the interstellar reddening from these data $E(b - y) = 0.06 \pm 0.01$, corresponding to $E(B - V)_J = 0.08 \pm 0.01$. We derived $T_1 = 11300$ K and $T_2 = 6470$ K from Popper (1980) and Flower (1996) calibrations.

Both results are in good agreement. As the data for the secondary component in Table 1 have large errors, we accepted the temperature of the secondary $T_2 = 6500$ K, obtained from the LCs solutions (see Table 2).

For DX Vel we can find the temperature of the primary component from 3 independent sources.

i) We estimated the interstellar reddening from the two-colour diagram in Fig. 2 as $E(V - B)_W = 0.0164$. From $(V - B)_{0W} = 0.0708$ and Lub & Pel (1977) calibration we obtained $T_1 = 8040$ K and $\log g = 4.0$. Transforming Walraven magnitudes into the Johnson system according to (2) we got $E(B - V)_J = 0.04$. The $(B - V)_{0J} = 0.198$ and Flower (1996) calibration suggest the temperature of the primary component equal to 7780 K or even 7710 K using the Popper (1980) calibration.

ii) We used $uvby, \beta$ photometry of Wolf & Kern (1983). Due to the fact that only one observation on the plateau was obtained ($b - y = 0.137$, $m1 = 0.190$, $c1 = 0.923$) we can find only the temperature for combined light. The use of calibrations by Breger (1974) for the $uvby, \beta$ photometry gives after correction for interstellar reddening $E(b - y) = 0.03$, corresponding to $E(B - V)_J = 0.04$, the temperature for combined light 7900 K, $\log g = 3.95$ and solar abundance.

iii) We used a low resolution ($R = 5960$) spectrum of DX Vel obtained with the VISTA 4m telescope by Tiago Ribeiro (Volkov et al., 2013). We derived from our spectrum the temperature 8000 K with $\log g = 4.5$ by comparing it with the POLLUX Database of Stellar Spectra (Palacios et al., 2010). The $\log g$ affects the width of hydrogen lines. As seen in Fig. 2 of the paper Volkov et al.

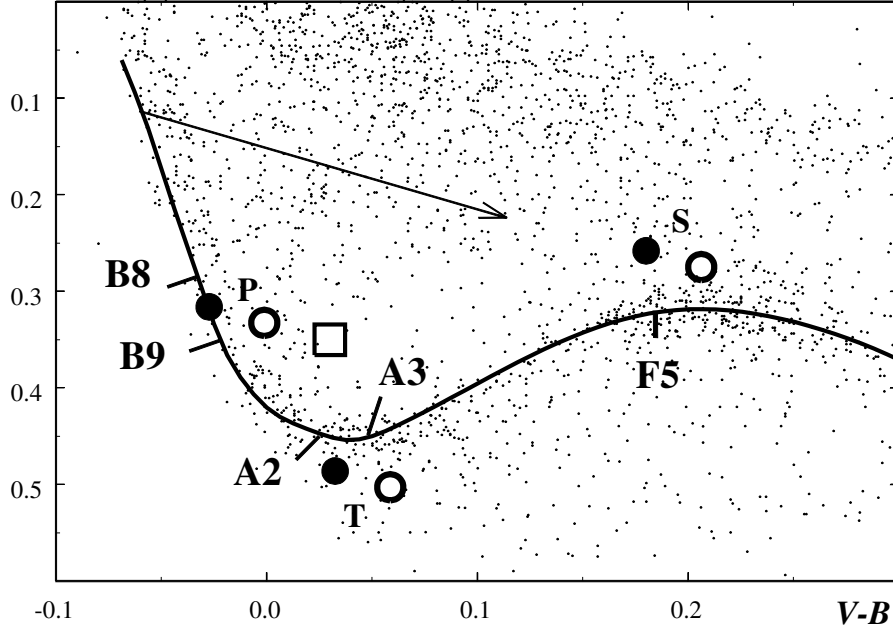
B-U

Figure 1. The $(B - U)_W, (V - B)_W$ diagram for RW CrA. The arrow stays for the direction of the interstellar reddening. The solid line - standard main sequence from Walraven & Walraven (1977), the points - observations in the Walraven system from Nitschelm & Mermilliod (1990) catalogue. The open square marks the color indices of the combined light. Observed and dereddened indices of the primary (P), secondary (S) and tertiary (T) components are represented by open and full circles, respectively.

(2013), they are very strong in our spectrum. Its low resolution and the same spectral type of the primary and tertiary component did not allow to distinguish them in the combined spectrum. The secondary component is too faint to be detected. It provides less than 5% of the combined light at 5500\AA .

We accepted the temperature of the primary component of DX Vel $T_1 = 7950\text{ K}$ as a reasonable compromise between all photometric and one spectral estimations.

The binary V0646 Cen displays a very deep primary minimum with the flat bottom, when only the dim secondary component is observed. So it is very simple to disentangle the colour indices of the components (see Table 1). The position of the components in a two colour diagram is shown in Fig. 3. This diagram enables us to find the interstellar reddening. We derived $E(V - B)_W = 0.0279$ and converting the Walraven magnitudes into the Johnson system according to (2)

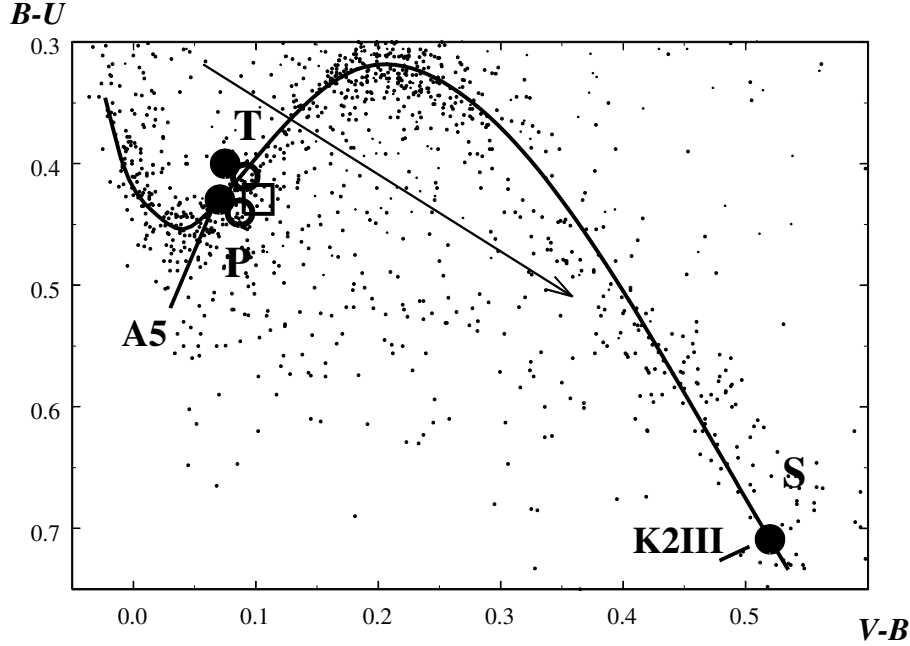


Figure 2. The $(B-U)_W, (V-B)_W$ diagram for DX Vel. The position of the secondary component corresponds to its temperature and luminosity class from Table 2. The description of other symbols is the same as in Fig. 1.

as $E(B-V)_J = 0.074$. From Flower (1996) calibration we obtain $T_1 = 13500$ K (Sp=B6) and $T_2 = 6180$ K (Sp=F8). The spectral class obtained from our photometry is more earlier than B8IV given in the SIMBAD database.

There are two $uvby, \beta$ measurements of the object (Wolf & Kern, 1983). Both of them were taken at the bottom of the primary minimum and seemed referred to the secondary component. But the first one gives improbable colour indices, so we consider it erroneous. The second one, according to our new ephemeris, refers to the ascending branch of the LC where approximately 20% of the light belongs to the primary component. So these measurements are useless.

4. Absolute parameters and ETV diagrams

The LCs of all three binaries show proximity effects. So we used the PHOEBE program of Prša & Zwitter (2005) for their analysis. We have got an individual solution for every source of data and then we took mean weighted values for the parameters.

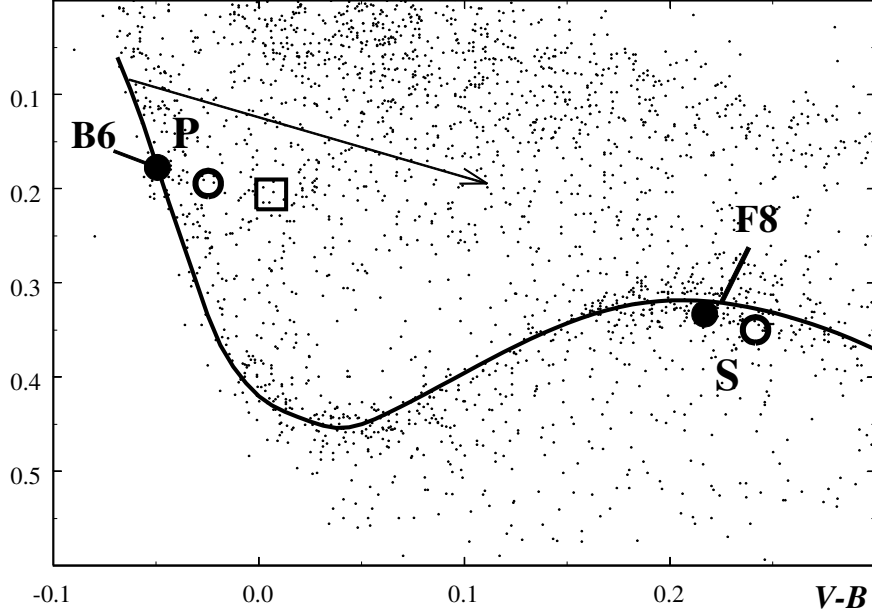
B-U

Figure 3. The $(B-U)_W, (V-B)_W$ diagram for V0646 Cen. The description of symbols is the same as in Fig. 1.

Table 1. The colour indices of the components in the Walraven and Johnson systems and their spectral types.

Star	$(V-B)_W$	$(B-U)_W$	$(B-V)_J$	$E(B-V)_J$	Sp
RW CrA, P	-0.0011 ± 0.0007	0.3326 ± 0.0009	-0.011 ± 0.018	0.08 ± 0.01	B8
RW CrA, S	0.206 ± 0.009	0.275 ± 0.014	0.51 ± 0.04	"	F5
RW CrA, T	0.0277 ± 0.0010	0.4407 ± 0.0010	0.065 ± 0.0	"	A2
DX Vel, P	0.0962 ± 0.0009	0.4425 ± 0.0009	0.240 ± 0.009	0.04 ± 0.01	A5
DX Vel, S	-	-	-	"	K4
DX Vel, T	0.0915 ± 0.0015	0.4109 ± 0.0019	0.186 ± 0.010	"	A5
V0646 Cen, P	-0.0246 ± 0.0007	0.1945 ± 0.0009	-0.073 ± 0.018	0.07 ± 0.01	B6
V0646 Cen, S	0.2417 ± 0.0010	0.3499 ± 0.0015	0.598 ± 0.009	"	F8

P - primary, S - secondary, T - tertiary

All available LCs were solved and the resulting parameters (the mass ratio q , the inclination i , the effective temperature T , the fractional radius r , the potential Ω and the third light L_{3V}) are presented in Table 2. The temperatures of the primary components of all 3 systems, determined in Section 2, were fixed in our solutions. The temperatures of the secondary components were found from PHOEBE solutions and for RW CrA and V0646 Cen they are within the errors, in agreement with those found in Section 2. The temperatures of the third components in RW CrA and DX Vel were found from the third light in PHOEBE solutions and are in agreement with results of Section 2, too. The LCs solutions in all passbands provide also luminosities of the components. For simplicity, we present only the third light L_{3V} in RW CrA and DX Vel, supposing $L_1 + L_2 + L_3 = 100\%$.

The absolute parameters of all 3 systems are presented in Table 3. We found the masses of the components by a non-direct method first described by Khalullin (1985), which is based on an empirical mass-luminosity relation, the 3rd Kepler law and the relation between the absolute and relative radius:

$$\begin{aligned}\log(L_1/L_\odot) &= 3.99 \log(M_1/M_\odot), \\ a^3/P^2 &= M_1(1+q), \\ R_1 &= r_1 a.\end{aligned}\tag{2}$$

While the light curves' solution for semidetached systems provides a reliable value of q , in the case of detached systems we have to derive q using the formula:

$$q = M_2/M_1 = (L_2/L_1)^{1/3.99} = ((T_2/T_1)^4 (r_2/r_1)^2)^{1/3.99}.\tag{3}$$

An independent determination of the temperatures of the components are of paramount importance. The described method of determination of absolute parameters of the binaries by a semi-empirical way can be applied in the case that radial velocity curves of the components are not available.

To derive the precise minima times from photoelectric and CCD observations, we fitted the synthetic LCs through individual observations by means of the PHOEBE program. In the case of simultaneous observations in several filters the minima times were weighted and mean values were calculated. The minima times are listed in Tables 4, 6, 7, together with already published ones. All three systems have much more luminous primary components. The shallow secondary minima are due to their lower precision not suitable for a period analysis. Therefore, only primary minima times were used to construct the ETV diagrams. The time interval of ASAS observations, taken during almost 9 years, was divided into shorter intervals for DX Vel and V0646 Cen and normal minima for each interval were calculated. For RW CrA the uneven distribution of ASAS points allowed us to obtain only one precise normal minimum time.

The physical parameters of the third bodies were supposed from the distances, temperatures and luminosities, estimated in this investigation, with the help of obvious formulae:

$$\begin{aligned}
M_{V,3} &= V_3 - 3.1E(B - V)_J + 5 + 5 \log \pi, \\
M_3 &= M_{V,3} + B.C._3, \\
\log(L_3/L_\odot) &= 0.4(M_\odot - M_3), \\
\log(L_3/L_\odot) &= 2 \log(R_3/R_\odot) + 4 \log(T_3/T_\odot).
\end{aligned} \tag{4}$$

The bolometric correction $B.C.$ was found from the Flower (1996) calibration and the accepted bolometric magnitude of the Sun $M_{bol_\odot} = 4.74$ as proposed by IAU 2015 Resolution B2. The mass of the third component was estimated from the empirical mass-luminosity relation of Torres et al. (2010). The gravitational acceleration was found assuming $\log g_\odot = 4.44$. The parameters of the third bodies seem to be quite reliable. They evolved as single stars and have no influence on the evolution of the binaries.

In all solutions we prefer the linear darkening coefficients. Non-linear darkening laws did not improve the $O - C$ scatter. The linear darkening coefficients were derived through van Hamme (1993) tables by the PHOEBE program. They can be found from temperatures and gravitational accelerations of the components, so we did not put them into Table 2. We assumed bolometric albedos equal to 0.6 as recommended by PHOEBE. Gravity darkening coefficients of the components of binaries were taken from Alencar & Vaz (1997) according to their temperatures and chemical composition (assumed solar, as it does not have significant influence on their light curves). Therefore, for the primary and secondary components of our binaries we accepted the value of gravity darkening coefficient $\beta = 1.0$ and $\beta = 0.32$, respectively. Variation of these parameters did not show any improvements in the solutions of the LCs.

Table 2. The parameters derived from Walraven photometry and LCs fittings.

Parameter	RW CrA	DX Vel	V0646 Cen
i [$^\circ$]	89.54 ± 0.05	$83.0 - 85.1$	88.57 ± 0.04
type of binary	detached	semidetached	semidetached
$q(M_2/M_1)$	0.59 ± 0.03	0.482 ± 0.007	0.428 ± 0.001
T_1 [K] (fixed)	11100 ± 150	7950 ± 100	13500 ± 300
T_2 [K]	6500 ± 80	4460 ± 70	6080 ± 100
T_3 [K]	8700 ± 200	8030 ± 100	-
r_1	0.334 ± 0.001	0.238 ± 0.002	0.208 ± 0.002
r_2	0.301 ± 0.002	0.318 ± 0.003	0.309 ± 0.002
Ω_1	3.04 ± 0.01	2.84 ± 0.01	2.74 ± 0.01
Ω_2	2.70 ± 0.02	2.55 ± 0.01	2.48 ± 0.01
L_{3V} (%)	18.7 ± 0.2	40.1 ± 0.3	-

Table 3. The absolute parameters derived by a non-direct method.

Parameter	RW CrA	DX Vel	V0646 Cen
M_1 [M_\odot]	3.6 ± 0.2	1.7 ± 0.2	3.9 ± 0.2
$q(M_2/M_1)$	0.56 ± 0.03	-	-
R_1 [R_\odot]	3.5 ± 0.2	1.5 ± 0.2	2.7 ± 0.2
R_2 [R_\odot]	3.2 ± 0.2	1.9 ± 0.1	3.9 ± 0.2
$\log g_1$	3.90 ± 0.03	4.33 ± 0.03	4.18 ± 0.01
$\log g_2$	3.73 ± 0.03	3.76 ± 0.03	3.47 ± 0.01
$\log g_3$	3.92 ± 0.05	4.44 ± 0.03	-
d [pc]	1050 ± 100	550 ± 70	675 ± 50

4.1. RW CrA

We solved the photometric LCs of RW CrA with the fixed temperature of the primary component $T_1 = 11100$ K. The parameters of the system are presented in Table 2. The V LC fit and residuals from the LCs fits in other passbands, Hipparcos and ASAS data are shown in Fig. 4. Geometric elements r_1, r_2, i of our solution are in full agreement with the values found by Grygar & Horak (1980).

Using the amount of the third light in the solutions in different passbands, we obtained the third light colour indices presented in Table 1. Taking into account interstellar reddening $E(V - B) = 0.0288$, we found the temperature of the third component $T_3 = (8700 \pm 200)$ K with the help of calibration from Lub & Pel (1977). This enables us to get from (1) the size of the star $R_3 = 2.71R_\odot$ and from the empirical mass-luminosity relation of Torres et al. (2010) the values of $M_3 = 2.23 M_\odot$ and $\log g_3 = 3.92 \pm 0.05$. The position of all three stars in the $(B - U)_W, (V - B)_W$ diagram is given in Fig. 1. The existence of a third massive component takes responsibility for a large third light found first by Grygar & Horak (1980). The other problem is that the secondary on a two-colour diagram (Fig. 1) has an UV excess that could be assigned to a metal deficiency of this star, but the error of determination of the colour index of the secondary is so large that it does not allow to make any conclusion about the chemical composition of the star.

Giesekeing (1976) obtained the radial velocity curve of RW CrA with the 0.4m Grand Prism Objective refractor in La Silla (ESO) using the Fehrenbach prism. The declared in that work value of $K_1 = 65$ km/s is too small for the expected value of $K_1 = 158$ km/s from our solution. Our attempt to find the LCs solution for $q = M_2/M_1 = 0.46$, corresponding to $K_1 = 65$ km/s, failed. Due to the fact, that the primary component B8 and the third component A2 are both characterized by strong hydrogen lines, it seems that they were not resolved in objective prism spectra, which led to the lower value of the semiamplitude of the RV curve $K_1 = 65$ km/s. The spectrum of the RW CrA in the Houk (1982)

catalogue is marked as B8/A0III. These spectral types are close to the spectral types derived by us photometrically for the primary and tertiary components. As seen in Table 1, the spectrum of the secondary component is F5 and could not be confused with the spectral type A2.

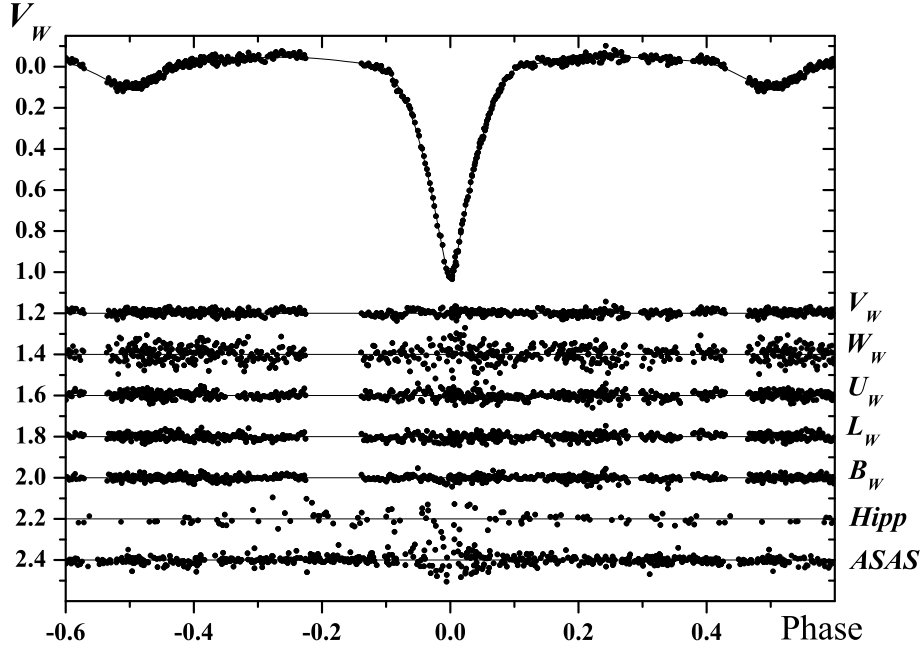


Figure 4. Van Houten's RW CrA V_W observations with the best fit and the residuals of V_W, W_W, U_W, L_W, B_W , Hipparcos and ASAS data after the best fits using the parameters from Table 2.

Using the data from Table 2 we varied only the epochs of observations and obtained the individual minima times with the PHOEBE program for van Houten's, ASAS, Hipparcos, Mallama (1981) and our own data. We added all minima times found in the literature and minima found in this work (TW). The results are presented in Table 4. The $O - C$ residuals in the ETV diagram (Fig. 5) and in Table 4 were calculated using the linear ephemeris:

$$\text{HJD Min I} = 2438987.453 + 1.6836009 \times E. \quad (5)$$

The residuals from this formula were fitted by the LITE orbit. Parameters of this orbit, mass function of the triple system and the estimation of the third body mass are given in Table 5. Taking into account the estimated mass of the third component $M_3 = 2.23 M_\odot$, we obtained the inclination of the third body

Table 4. Times of minima for RW CrA.

HJD – 2400000	Epoch	Residuals from linear ephemeris (5)	Remarks
31017.297(9)	-4734	0.0107	Ponsen (1954)
38987.4477(1)	0	-0.0053	van Houten et al. (2009), TW
43342.9212(5)	2587	-0.0073	Kvíz (1979)
44435.5945(4)	3236	0.0092	Mallama (1981)
44462.5323	3252	0.0092	Wolf et al. (1982)
48745.6082(10)	5796	0.0044	Hipparcos, TW
53528.7069(4)	8637	-0.0071	ASAS, TW
54161.7400(12)	9013	-0.0079	Zasche (2010)
57230.9457(3)	10836	-0.0066	Pavlov et al. (2016)
57579.4559(2)	11043	0.0018	TW

Table 5. Parameters of the third body orbits

	RW CrA	DX Vel
P_3 (period) [days]	13590(50)	28840(200)
P_3 (period) [years]	37.2(2)	78.9(5)
T_0 (time of periastron) [JD]	2457680(100)	2457670(200)
$a_3 \sin i$ [au]	4.57(3)	1.13(13)
e	0.93(1)	0.84(3)
ω [°]	4.5(5)	223.5(30)
$f(M)_3$ [M_\odot]	0.068	0.00023
M_3 [M_\odot]	2.2(3)	1.1(2)
i [°]	46(4)	8(3)

orbit to the line of sight $i = 46^\circ \pm 4^\circ$. The semi-major axis of the third body orbit is $A_3 = 22$ au. The mean deviation of the residuals from the theoretical fit $\pm 0^d.0004$ is close to the mean error of minima times $\sigma = \pm 0^d.0005$ given in the first column of Table 4, except the photographic one. The larger scatter of ASAS residuals in Fig. 4 may be caused by the changes of the orbital inclination i with time due to the possible precession of the orbit that follows from noncoplanarity of the orbits. Other LCs do not show such an effect, but they were obtained in shorter time intervals than 7.5 years of the ASAS observations. For further investigation of possible i variations with time one should assign the mean time of van Houten’s observations for the value of i given in Table 2.

4.2. DX Vel

Our first analysis of the system supposed the detached mode (Volkov et al., 2013). As seen in Fig. 1 of that paper, the star has a small $U - B$ ultraviolet

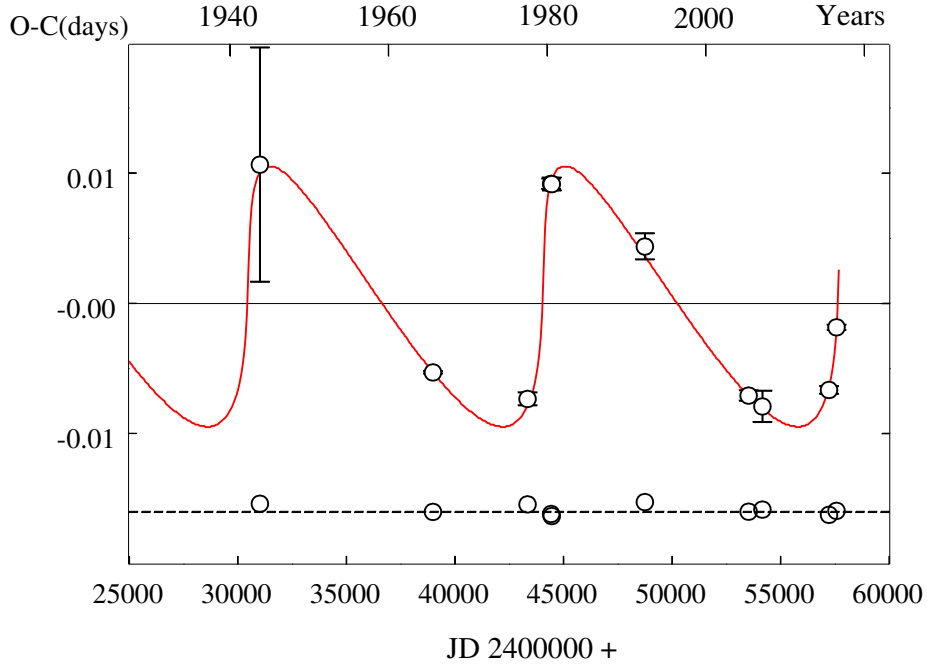


Figure 5. The ETV diagram for RW CrA, constructed using the ephemeris (5), fitted by a LITE curve (top) and their residuals after the subtraction of the adopted solution (bottom).

excess in the primary minimum when the hot primary component is occulted by the cooler secondary. Such excess in the dominant A-spectrum can be explained by another star with a little bit higher UV luminosity. So the possible explanation for this anomaly can be the existence of the third body in the system, best visible in a combined spectrum during the primary eclipse when the light of the primary component is suppressed. As shown in Fig. 2, the position of the object (combined light) in the $(B - U)_W$, $(V - B)_W$ diagram is above the position of the primary component.

Furthermore, the new solution in the semidetached mode with the secondary component filling its Roche lobe allows as much as 40% of the third light in the system in all bands. Inspection of the SDSS images reveals a dim red optical companion of the star with the angular distance of $5.6''$, which cannot provide extra light with such characteristics. So we can suppose presence of the third star in the system with the temperature nearly equal to that of the primary component. The question is if it is gravitationally bound with the double. Our previous investigation of positions of all available primary minima times in the ETV diagram revealed orbital period changes (Volkov et al., 2013). The position

of minima could be approximated either by a parabola or the LITE orbit almost equally well. We continued observations and made a more detailed analysis of all available LCs. We found a combination of parameters in a semidetached mode, which satisfy the light LCs in all passbands much better than in the detached mode. It allows a larger amount of the third light and provides more suitable physical parameters of the components than in the detached mode. In the semidetached mode the light between minima changes by a combination of a reflection effect and ellipticity and in the detached mode mainly by ellipticity. The residual deviations are smaller in the semidetached mode. Our new observations proved that the depths of minima change with time. We were able to reconcile all observations by the same set of parameters in the semidetached mode varying only the inclination i of the orbit. In the detached mode all parameters have to be changed to find the best fit in different bands and different data sets. The reason of the changes in minima depths could be the precession of the orbit of the eclipsing binary as the orbits of the binary and the third body are not coplanar. We obtained 4 estimates of the orbital inclination in 4 independent epochs:

van Houten, $i = 83.79^\circ \pm 0.08^\circ$, apastron of the third body,
 ASAS, HJD 2452578, $i = 82.78^\circ \pm 0.09^\circ$, intermediate position,
 ASAS, HJD 2454482, $i = 83.10^\circ \pm 0.11^\circ$, intermediate position,
 our observations, $i = 85.11^\circ \pm 0.08^\circ$, periastron of the third body.

We present the mean weighted parameters for solutions of different observational sets for the semidetached mode in Table 2. The LC in V_W with the best fit and residuals from the best fits of available data, using the parameters from Table 2, are shown in Fig. 6.

Using this mode we varied only the epochs of observations in order to obtain the individual minima times with the PHOEBE program. The results are presented in Table 6.

Available 8 photographic minima times by van Houten (1950) and Hoffmeister (1949) were reduced to a single epoch named "photographic" to calculate one normal time of the primary minimum with a suitable precision. The ASAS data were divided into 2 intervals. The $O - C$ residuals in the ETV diagram in Fig. 7 and Table 6 were calculated using the linear ephemeris:

$$\text{HJD Min I} = 2\,443\,583.4618 + 1.11730365 \times E. \quad (6)$$

The residuals from this formula were fitted by the LITE orbit. Parameters of this orbit and the mass function of the triple orbit are presented in Table 5.

Using the amount of the third light in the solutions in different passbands we obtained the third light colour indices given in Table 1. Taking into account interstellar reddening $E(V - B)_W = 0.0164$ we got the temperature of the third component $T_3 = (7860 \pm 100)$ K from the Flower (1996) calibration. It is 80 K higher than the temperature of the primary component obtained by the

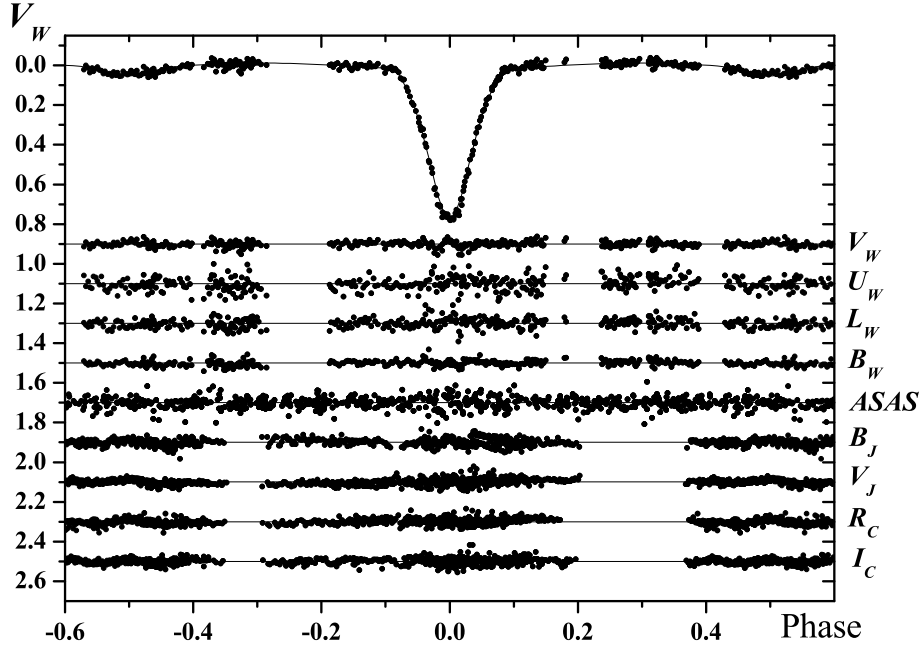


Figure 6. Van Houten's DX Vel V_W observations with the best fit and the residuals of V_W, U_W, L_W, B_W , ASAS and our B, V, R_C, I_C data after the best fits using the parameters from Table 2.

Table 6. Times of minima for DX Vel.

HJD - 2400000	Epoch	Residuals from linear ephemeris (6)	Remarks
29037.280(8)	-13019	-0.0056	photographic, TW
43583.4660(2)	0	+0.0042	van Houten et al. (2009), TW
52578.8772(3)	8051	+0.0037	ASAS, TW
54482.7603(3)	9755	+0.0013	"
56051.4533(10)	11159	+0.0000	TW
56053.6873(2)	11161	-0.0006	"
56080.5032(2)	11185	+0.0000	"
56292.7906(2)	11375	-0.0003	"
56739.7107(1)	11775	-0.0016	"
56748.6486(2)	11783	-0.0021	"
57378.8063(1)	12347	-0.0037	"
57386.6273(1)	12354	-0.0038	"

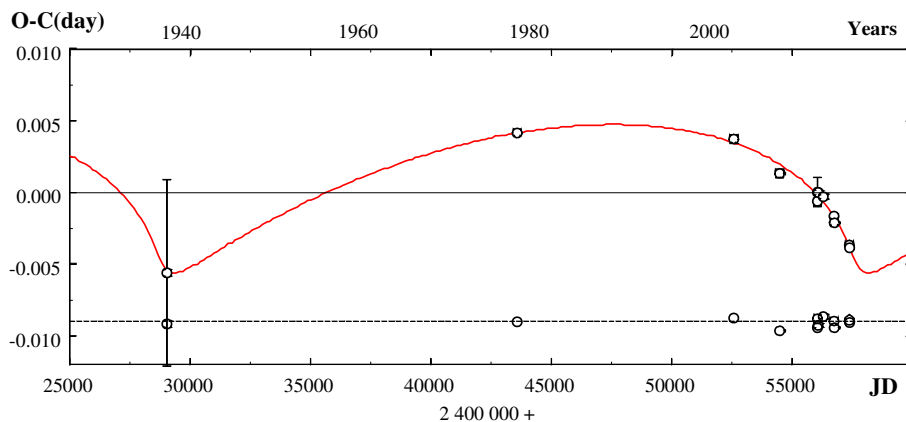


Figure 7. The ETV diagram for DX Vel, constructed using the ephemeris (7), fitted by a LITE curve (top) and their residuals after the subtraction of the adopted solution (bottom).

same method. The difference in temperatures of the components can be derived more precisely than the temperature alone, so we accept this difference in stars' temperatures and give for the third component the value $T_3 = 8030$ K (see Table 2). This enables us to get from (1) the size of the tertiary component as $R_3 = 1.22R_\odot$. From the empirical mass-luminosity relation of Torres et al. (2010) we suggested $M_3 = 1.1 M_\odot$ and $\log g_3 = 4.29 \pm 0.05$. The conditions for a detection of the spectrum of the third component are most favorable in the modern epoch as the relative speed of the stars is maximal. From the estimation of the third body mass we found the inclination of the orbit of the third body to the line of sight as $i = 8^\circ \pm 3^\circ$. The semi-major axis of the third body orbit is 28 au. During the next 30 years the angular distance of the components will increase from $0.02''$ to $0.05''$. Due to the fact that in the recent epoch the binary passes the periastron of the third body orbit, we urge to continue photometric observations to get as many minima times as possible.

4.3. V0646 Cen

The binary has a very deep primary minimum, so the precision of determination of minima times, listed in Table 7, is very high. Numerous photographic observations taken by O'Connell (1956) during 20 years were divided into two intervals. For each interval the normal minimum was derived. The same procedure was used for ASAS observations. The time interval of observations close to 9 years was divided into three intervals, see Table 7. Van Houten's observations were taken during 2.5 months, so it is reasonable to define one very precise normal minimum for these data. The secondary component fills its Roche lobe

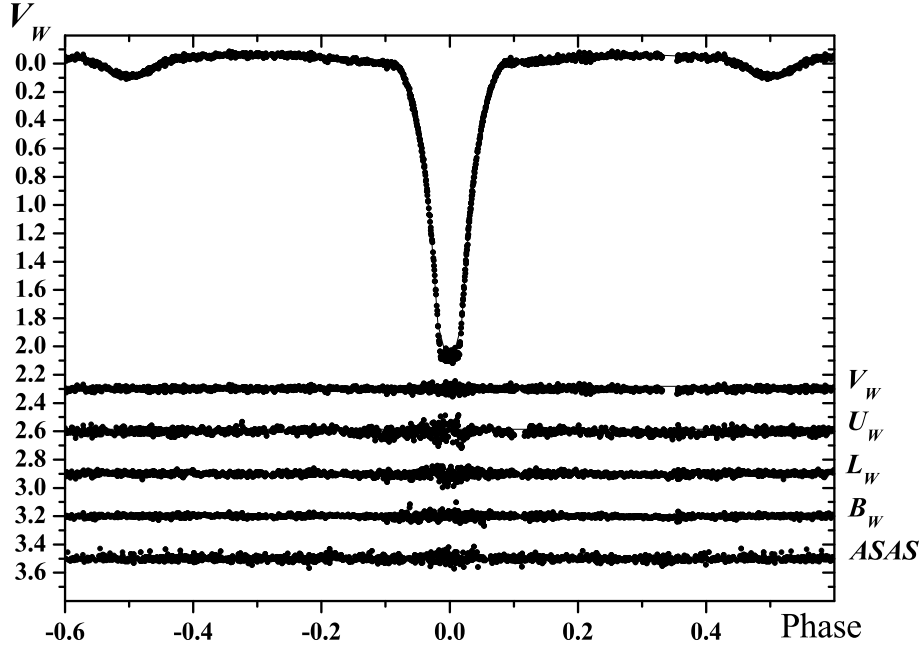


Figure 8. Van Houten's V0646 Cen V_W observations with the best fit and the residuals of V_W , U_W , L_W , B_W , ASAS after the best fits using the parameters from Table 2.

and the mass transfer should be responsible for the period change. Van Houten noted that the levels of the optical flux just before and after the primary minimum are little bit different and it can be assigned to the matter flows in the system. We constructed an ETV diagram using the ephemeris related to the well-determined minimum from van Houten's observations:

$$\text{HJD Min I} = 2\,439\,937.5140 + 2^d.24657335 \times E. \quad (7)$$

The minima times in the ETV diagram can be fitted by a parabola (continuous period change), represented by the following ephemeris:

$$\text{HJD Min I} = 2\,439\,937.5139(3) + 2^d.24657289(9) \times E + 7.22(4) \cdot 10^{-11} \times E^2. \quad (8)$$

The weights for the minima times were taken as $1/\sigma^2$. A continuous increase of the orbital period can be interpreted by a conservative mass transfer from the secondary to the primary component at the rate of $\dot{M} = 6.08 \times 10^{-9} M_\odot/\text{yr}$. This value was calculated using the orbital period change (8), the masses of the components from Table 2 and a well-known relation (e.g., Pribulla (1998)).

Table 7. Times of minima for V0646 Cen.

HJD – 2400000	Epoch	Residuals from linear ephemeris (7)	Remarks
28369.9112(6)	-5149	0.0033	O’Connell (1956), TW
32651.8793(5)	-3243	0.0026	O’Connell (1956), TW
39937.5139(1)	0	-0.0001	van Houten et al. (2009), TW
43916.1946	1771	-0.0008	Kvíz (1979), *
52704.7898(2)	5683	-0.0006	ASAS, TW
53468.6248(2)	6023	-0.0005	”
54589.6648(3)	6522	-0.0006	”
56321.7746(2)	7293	0.0011	TW
56519.4723(4)	7381	0.0004	”
57451.8002(2)	7796	0.0004	”

* the standard error was not published

O-C, days

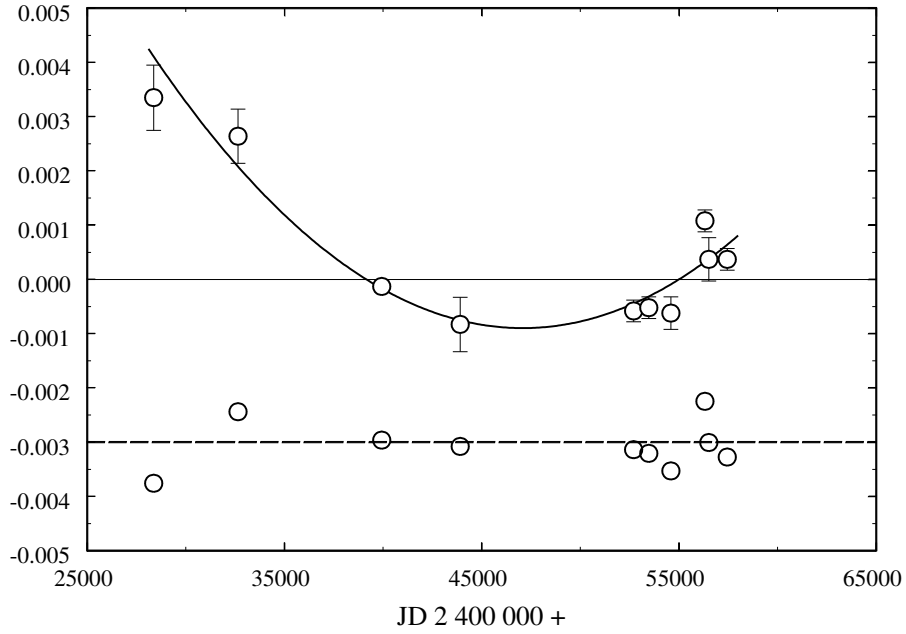


Figure 9. The ETV diagram for V0646 Cen, constructed using the ephemeris (7), fitted by a parabola (8) (top) and residuals from this fit (bottom).

5. Interstellar reddening - comparison with surveys

We derived interstellar reddening from $(B - U)_W, (V - B)_W$ diagrams and compared the results with the data from available surveys. Unfortunately, a new review of interstellar absorption (Green et al., 2015) has a gap on the positions of all three stars.

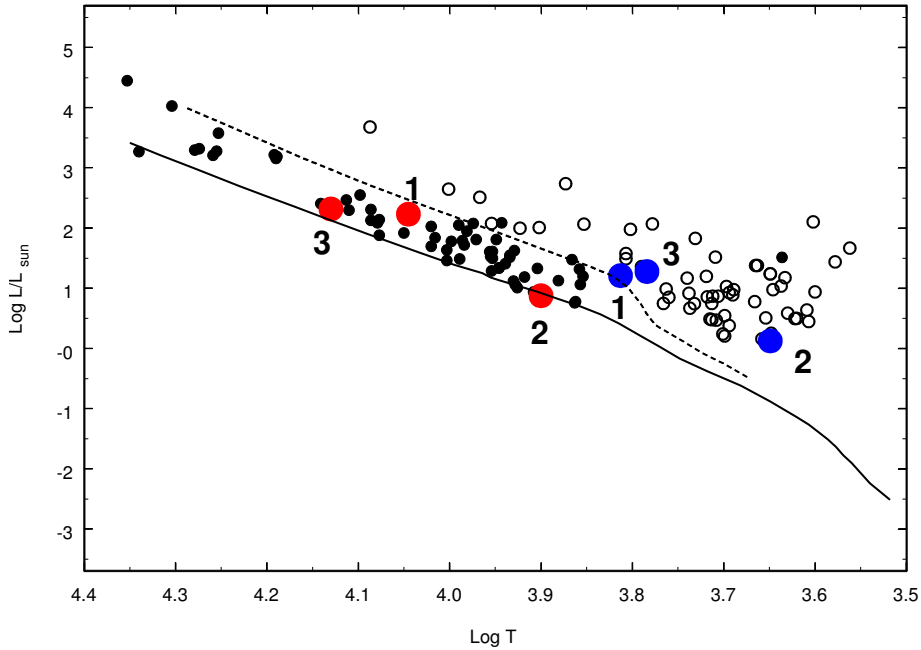


Figure 10. Location of primary (filled circles) and secondary components (open circles) in the HR diagram for semidetached Algol binaries, taken from Ibanoglu et al. (2006). Continuous and dashed lines represent the ZAMS and TAMS for solar chemical abundance (Girardi et al., 2000), respectively. We added the location of the primary (red circles) and secondary components (blue circles) of RW CrA (1), DX Vel (2) and V0646 Cen (3). (A colour version of this figure is available in the online journal.)

The objects RW CrA and DX Vel are situated close to the Galactic plane with the galactic latitudes $b = -7.0^\circ$ and $b = 2.5^\circ$ for RW CrA and DX Vel, respectively. Therefore, we expect a significant reddening for both objects taking into account their distances 1050 pc and 550 pc (see Table 3). The surveys of Schlafly & Finkbeiner (2011) and Schlegel et al. (1998), with the use of a formula from Bonifacio et al. (2000), which takes into account the distance of the object, give the mean interstellar reddening $E(B - V)_J = 0.14$ and $E(B - V)_J = 0.12$

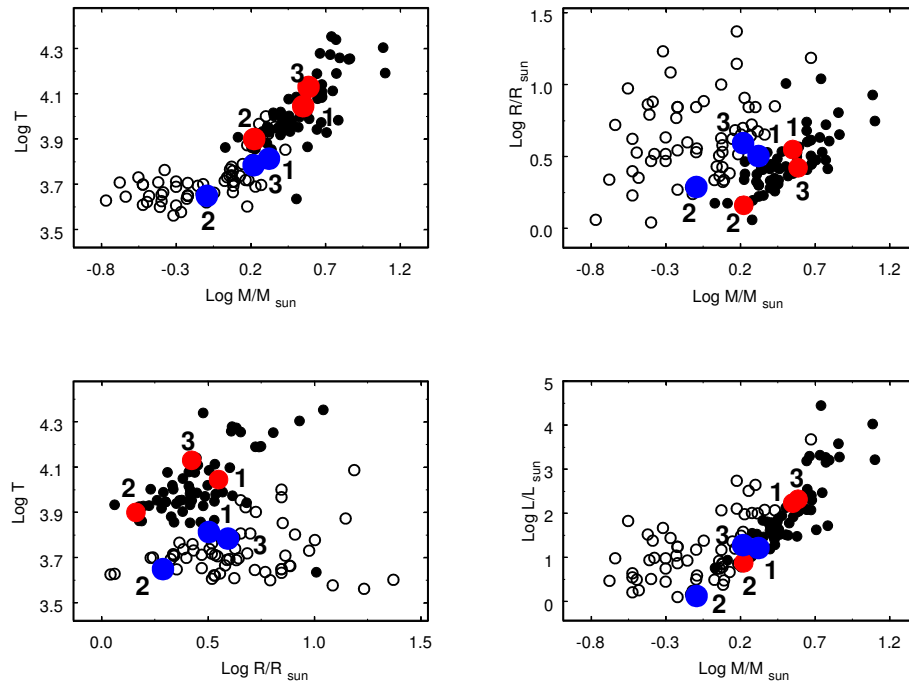


Figure 11. Various diagrams for semidetached Algol binaries taken from Ibañoğlu et al. (2006). Symbols are the same as in Fig. 10.

for RW CrA and DX Vel, respectively. Both values are larger than it follows from photometric measurements (see Table 1).

Kraft & Landolt (1959) suggested that DX Vel is a member of Collinder 213 (C213) open cluster. According to WEBDA (<http://webda.physics.muni.cz>), its interstellar reddening and distance are $E(B - V)_J = 0.07$ and 1400 pc, respectively. DX Vel lies 19.5' from the cluster centre. Our estimate of the distance of DX Vel of 550 pc excludes it as a member of the cluster. The interstellar reddening in the direction of C213 is also lower than it follows from the surveys and confirms our estimate of the interstellar reddening.

V0646 Cen. The surveys give $E(B - V)_J = 0.10$, which is close to the photometric result.

6. Conclusions

We have found the reliable parameters of the southern Algol-type binaries RW CrA, DX Vel and V0646 Cen. Due to the lack of radial velocity data, the masses of their components were computed by a non-direct method. While RW CrA is a detached system, DX Vel and V0646 Cen are semidetached sys-

tems. Location of the primary and secondary components of RW CrA, DX Vel and V0646 Cen in the HR diagram and $\log T - \log M$, $\log R - \log M$, $\log T - \log R$, $\log L - \log M$ diagrams, are shown in Figs. 10 and 11.

The study of ETV diagrams enabled us to discover the presence of the third bodies in RW CrA and DX Vel with the periods of 37.2 years and 78.9 years, respectively. The changes in minima depths of both systems could be explained by long term variations of their orbital inclinations because their binary and third body orbits are not coplanar.

The detected orbital period increase in V0646 Cen binary can be explained by a mass transfer from the less to more massive component with the rate of $\dot{M} = 6.08 \times 10^{-9} M_{\odot}/\text{yr}$.

High resolution spectra of studied systems are needed to get the masses of components from radial velocity curves and to fix the γ -velocities variations in discovered triple systems. As the third bodies in RW CrA and DX Vel have recently passed periastrons and it seems that both orbits are precessing, photometric observations of the primary minima are badly needed, too.

Acknowledgements. This study was partly supported by the scholarship of the Slovak Academic Information Agency, the Slovak Research and Development Agency under the contract No. APVV-15-0458, the VEGA grant No. 2/0143/14. We would like also thank the Pierre Auger Collaboration for the use of its facilities. The operation of the robotic telescope FRAM is supported by the EU grant GLORIA (No. 283783 in FP7-Capacities program) and by the grant of the Ministry of Education of the Czech Republic (MSMT-CR LM2015038). The data calibration and analysis related to FRAM telescope is supported by the Ministry of Education of the Czech Republic MSMT-CR (LG15014 and CZ.02.1.01/0.0/0.0/16.013/0001402). We are grateful to our referee T. Pribulla for valuable suggestions and remarks leading to a significant improvement of the paper.

References

- Alencar, S. H. P. & Vaz, L. P. R. 1997, *Astron. Astrophys.*, **326**, 257
- Bonifacio, P., Monai, S., & Beers, T. C. 2000, *Astron. J.*, **120**, 2065
- Brancewicz, H. K. & Dworak, T. Z. 1980, *Acta Astron.*, **30**, 501
- Breger, M. 1974, *Astrophys. J.*, **192**, 75
- Budding, E. & Demircan, O. 2007, *Introduction to Astronomical Photometry* (Cambridge: Cambridge University Press)
- Budding, E., Erdem, A., Çiçek, C., et al. 2004, *Astron. Astrophys.*, **417**, 263
- Collaboration, T. P. A. 2015, *Nuclear Instruments and Methods in Physics Research Section A*, **798**, 172

- Ebr, J., Janeček, P., Prouza, M., et al. 2014, in *Revista Mexicana de Astronomia y Astrofisica Conference Series*, Vol. 45, 114–117
- Flower, P. J. 1996, *Astrophys. J.*, **469**, 355
- Gaposchkin, S. 1932, *Veroeffentlichungen der Universitaetssternwarte zu Berlin-Babelsberg*, **5**
- Gieseking, F. 1976, *Astron. Astrophys.*, **47**, 43
- Girardi, L., Bressan, A., Bertelli, G., & Chiosi, C. 2000, *Astron. Astrophys., Suppl. Ser.*, **141**, 371
- Green, G. M., Schlafly, E. F., Finkbeiner, D. P., et al. 2015, *Astrophys. J.*, **810**, 25
- Grygar, J. & Horak, T. B. 1980, *Bulletin of the Astronomical Institutes of Czechoslovakia*, **31**, 297
- Hoffmeister, C. 1949, *Erg. Astron.Nachr.*, **12**, A28
- Horak, T. B. 1975, *Bulletin of the Astronomical Institutes of Czechoslovakia*, **26**, 257
- Houk, N. 1982, Michigan Catalogue of Two-dimensional Spectral Types for the HD stars. Volume 3. Declinations $-40^{\circ}0$ to $-26^{\circ}0$. (MI(USA): Department of Astronomy, University of Michigan)
- Ibanoğlu, C., Soyduğan, F., Soyduğan, E., & Dervişoğlu, A. 2006, *Mon. Not. R. Astron. Soc.*, **373**, 435
- Khaliullin, K. F. 1985, *Astrophys. J.*, **299**, 668
- Kraft, R. P. & Landolt, A. U. 1959, *Astrophys. J.*, **129**, 287
- Kubánek, P., Jelínek, M., Nekola, M., et al. 2004, in *American Institute of Physics Conference Series*, Vol. 727, *Gamma-Ray Bursts: 30 Years of Discovery*, ed. E. Fenimore & M. Galassi, 753–756
- Kvíz, Z. 1979, *Information Bulletin on Variable Stars*, **1702**
- Lub, J. & Pel, J. W. 1977, *Astron. Astrophys.*, **54**, 137
- Malkov, O. Y., Oblak, E., Snegireva, E. A., & Torra, J. 2006, *Astron. Astrophys.*, **446**, 785
- Mallama, A. D. 1981, *Publ. Astron. Soc. Pac.*, **93**, 774
- Nitschelm, C. & Mermilliod, J. C. 1990, *Astron. Astrophys., Suppl. Ser.*, **82**, 331
- O’Connell, D. J. K. 1951, *Publications of the Riverview College Observatory*, **2**, 100
- O’Connell, D. J. K. 1956, *Ricerche Astronomiche*, **3**
- Palacios, A., Gebran, M., Josselin, E., et al. 2010, *Astron. Astrophys.*, **516**, A13

- Pavlov, H., Mallama, A., Loader, B., & Kerr, S. 2016, *Journal of the American Association of Variable Star Observers (JAAVSO)*, **44**, 26
- Pel, J. W. 1980, *Internal report Leiden Observatory*
- Perryman, M. A. C., Lindegren, L., Kovalevsky, J., et al. 1997, *Astron. Astrophys.*, **323**, L49
- Pojmanski, G. 2002, *Acta Astron.*, **52**, 397
- Ponsen, J. 1954, *Annalen van de Sterrewacht te Leiden*, **20**, 369
- Popper, D. M. 1980, *Ann. Rev. Astron. Astrophys.*, **18**, 115
- Pribulla, T. 1998, *Contributions of the Astronomical Observatory Skalnaté Pleso*, **28**, 101
- Prouza, M., Jelínek, M., Kubánek, P., et al. 2010, *Advances in Astronomy*, **2010**, 849382
- Prša, A. & Zwitter, T. 2005, *Astrophys. J.*, **628**, 426
- Schlafly, E. F. & Finkbeiner, D. P. 2011, *Astrophys. J.*, **737**, 103
- Schlegel, D. J., Finkbeiner, D. P., & Davis, M. 1998, *Astrophys. J.*, **500**, 525
- Soydugan, E., Soydugan, F., Demircan, O., & İbanoglu, C. 2006, *Mon. Not. R. Astron. Soc.*, **370**, 2013
- Torres, G., Andersen, J., & Giménez, A. 2010, *Astron. Astrophys. Rev.*, **18**, 67
- Torres, G., McGruder, C. D., Siverd, R. J., et al. 2017, *Astrophys. J.*, **836**, 177
- van Hamme, W. 1993, *Astron. J.*, **106**, 2096
- van Houten, C. J. 1950, *Annalen van de Sterrewachte Leiden*, **20**, 223
- van Houten, C. J., van Houten-Groeneveld, I., van Genderen, A. M., & Kwee, K. 2009, *Journal of Astronomical Data*, **15**
- Volkov, I. & Volkova, N. 2010, in *Astronomical Society of the Pacific Conference Series*, Vol. 435, *Binaries - Key to Comprehension of the Universe*, ed. A. Prša & M. Zejda, 323
- Volkov, I. M. 1990, *Information Bulletin on Variable Stars*, **3493**
- Volkov, I. M., Chochol, D., Grygar, J., et al. 2013, *Information Bulletin on Variable Stars*, **6066**
- Volkov, I. M., Chochol, D., Volkova, N. S., & Nikolenko, I. V. 2012, in *IAU Symposium*, Vol. 282, *From Interacting Binaries to Exoplanets: Essential Modeling Tools*, ed. M. T. Richards & I. Hubeny, 89–90
- Volkov, I. M., Volkova, N. S., Nikolenko, I. V., & Chochol, D. 2011, *Astronomy Reports*, **55**, 824
- Volkova, N. & Volkov, I. 2011, *Information Bulletin on Variable Stars*, **5976**
- Walraven, T. & Walraven, J. H. 1977, *Astron. Astrophys., Suppl. Ser.*, **30**, 245

Wolf, G. W. & Kern, J. T. 1983, *Astrophys. J., Suppl. Ser.*, **52**, 429

Wolf, G. W., Kern, J. T., Hayes, T. L., & Chaffin, C. R. 1982, *Information Bulletin on Variable Stars*, **2185**

Zasche, P. 2010, *Information Bulletin on Variable Stars*, **5931**